A Study on Characteristic Analysis of BLDC Motor Considering Various PWM Modes

Heung-Kyo Shin, *Tae Heoung Kim, Hwi-Beom Shin, and Soon-Young Lee
Department of Electrical Engineering, Gyeongsang National University, Jinju, Gyeongnam 660-701, Korea
*Corresponding Author (Phone: 82-55-751-5349 Fax: 82-55-759-2723 E-mail: ktheoung@gnu.ac.kr)

***Abstract*—Brushless DC motor (BLDCM) is driven by 120 degree square wave voltage and use PWM pulse patterns in two-phase feeding scheme to control the speed.**

In this paper, we propose the computational method for the BLDCM, which is driven by four PWM modes using time-stepped voltage source finite element method. And then we investigate motor characteristics at each PWM modes. According to a comparison based on each analysis result, we select a better PWM mode in the motor characteristics aspect. We also show that the proposed analysis method is appropriate to analyze a BLDC motor by comparing experimental results.

***Index Terms*—BLDCM, Finite Element Method, Permanent Magnet, Pulse Width Modulation.**

I. Introduction

Brushless DC motor (BLDCM) is a good candidate for most of the industrial applications and home appliances due to their distinct advantages over the induction machine [1][2]. It can be driven by alternating pulses of rectangular currents of 120 degree base and with a 120 degree shift between three phases of the stator. The pulse width modulation (PWM) pattern is commonly used in two-phase feeding scheme to control the speed of the motor, so it is possible to have various PWM modes in BLDCM control system [3].

In this paper, we introduce the numerical method using 2-dimensional time-stepped voltage source finite element method to analyze the influences of PWM modes on the performance of the BLDCM. According to a comparison based on each analysis result, we select a better PWM mode in the motor characteristics aspect. We also show that the proposed analysis method is appropriate to analyze a BLDC motor by comparing experimental results.

II. Analysis Model and PWM Modes

The 1/2 cross-sectional configuration of the interior-rotor type BLDC motor is outlined in Fig. 1. It has a six-pole stator and four-pole rotor. The permanent magnet material is sintered Ferrite. The air gap was designed to be 0.5 mm to obtain a reasonable permeance coefficient value. An encoder mounted on the shaft detects the rotor position and controls excitation of the appropriate stator phases.

Fig. 2 shows the drive circuit diagram of the BLDCM. The PWM pulse patterns that are used in this paper are U_ON-L_PWM, U_PWM-L_ON, ON-PWM, and PWM-ON mode as shown in Fig. 3. These alternate chopper controls were adopted to make the motor line current symmetrical and to distribute the switching losses in both the positive and negative side transistors.

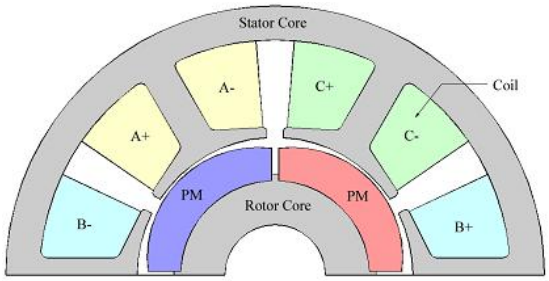

Fig. 1. The cross-section of BLDCM.

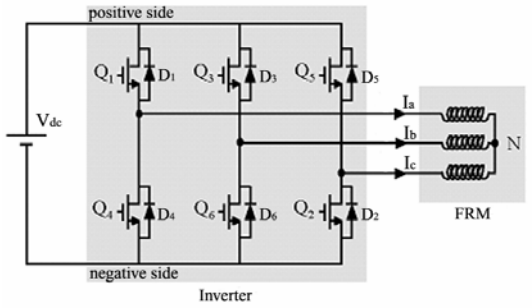

Fig. 2. The drive circuit diagram.

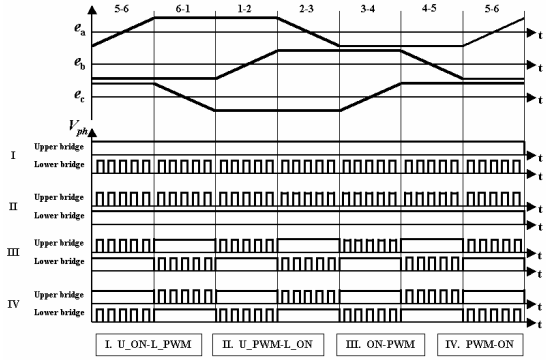

Fig. 3. BEMF and four PWM modes.

III. Finite Element Analysis

A. Governing Equation and Discretization

The 2-dimensional governing equation for the FRM is expressed in magnetic vector potential *A* by the following

$$\frac{\partial}{\partial x}\left(\frac{1}{\mu}\frac{\partial A_z}{\partial x}\right)+\frac{\partial}{\partial y}\left(\frac{1}{\mu}\frac{\partial A_z}{\partial y}\right)=-J_0-\frac{1}{\mu_0}\left(\frac{\partial M_y}{\partial x}-\frac{\partial M_x}{\partial y}\right) \quad (1)$$

where

A_z : Z component of magnetic vector potential

J_0 : Current density

M : Magnetization of the permanent magnet

Applying the Galerkin method to (1), we can obtain the finite element equation in a first order triangular element as follows:

$$I_{ie}=\int_{S^e}\frac{1}{\mu}\sum_{k=1}^{3}\left(\frac{\partial N_{ie}}{\partial x}\frac{\partial N_{ke}}{\partial x}+\frac{\partial N_{ie}}{\partial y}\frac{\partial N_{ke}}{\partial y}\right)A_{ke}\,dxdy$$
$$-\int_{S^e}\frac{1}{\mu_0}\left(M_x^e\frac{\partial N_{ie}}{\partial y}-M_y^e\frac{\partial N_{ie}}{\partial x}\right)dxdy \quad (2)$$
$$-\int_{S^e}J_0N_{ie}\,dxdy \qquad (i=1,2,3)$$

where N stands for shape function.

B. Consideration of Inverter Circuitry in PWM Modes

At each instant of time the interaction between the inverter circuitry and electromagnetics is achieved by defining the winding current in terms of the electrical circuit parameters [4][5]. The integration of the voltage equations must take account of the circuit topology, which changes at every commutation [6][7]. With reference to Figs 2 and 3, consider a 60-degree period when current is flowing through phases A and C. The switch Q1 and Q2 are turned on and off for PWM in this period, so the flow of current can be categorized into four cases in each PWM modes as shown in Fig. 4, 5, 6 and 7.

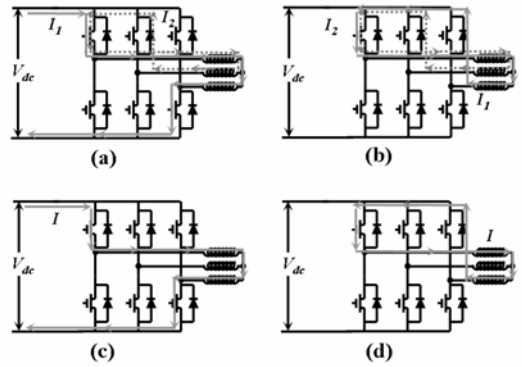

Fig. 4. The flow of current in the U_ON-L_PWM mode.

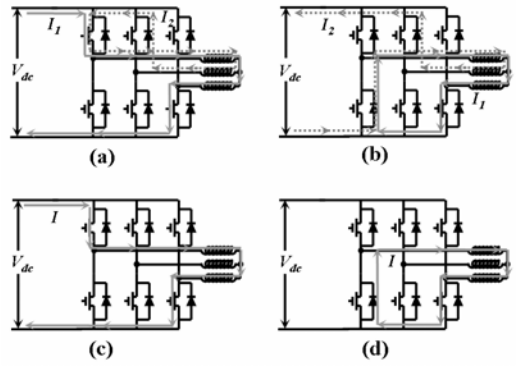

Fig. 5. The flow of current in the U_PWM-L_ON mode.

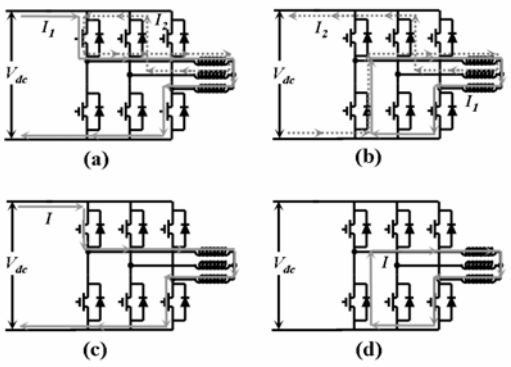

Fig. 6. The flow of current in the ON-PWM mode.

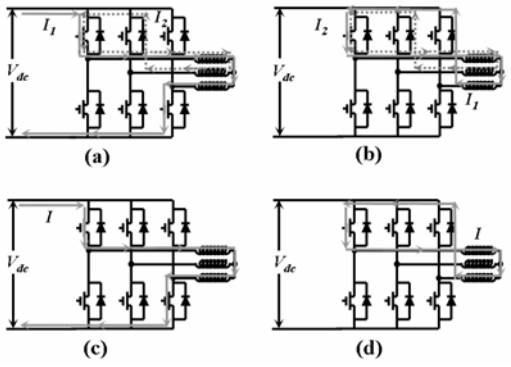

Fig. 7. The flow of current in the PWM-ON mode.

C. Voltage Equations

Fig. 4(a) and (b) show the flow of current in the U_ON-L_PWM mode at the commutation instant when switch Q_2 is on and off, respectively. In these cases, current continues to flow in open phase B because of its inductance L [8]. This current can be considered as a mesh current I2 that flows through diode D_3 and switch Q_1. The circuit voltage equation for I_2 may be written as:

$$RI_a+L_l\frac{dI_a}{dt}+\frac{d\Phi_a}{dt}+RI_b+L_l\frac{dI_b}{dt}-\frac{d\Phi_b}{dt}+V_{CE}+V_F=0 \quad (3)$$

where R is the resistance of phase winding, L_l is the leakage inductance of the stator coil ends, Φ is the flux linkage of phase winding, V_{CE} is the forward voltage drop across the transistor, and V_F is the voltage drop across the diode.

The main mesh current I_1 flows through switch Q_2 or diode D_5 according to the state of switch Q_2. The circuit voltage equations for each case can be obtained as follows:

$$RI_a+L_l\frac{dI_a}{dt}+\frac{d\Phi_a}{dt}+RI_c+L_l\frac{dI_c}{dt}-\frac{d\Phi_c}{dt}+2V_{CE}=V_{dc} \quad (4)$$

$$RI_a+L_l\frac{dI_a}{dt}+\frac{d\Phi_a}{dt}+RI_c+L_l\frac{dI_c}{dt}-\frac{d\Phi_c}{dt}+V_{CE}+V_F=0 \quad (5)$$

where V_{dc} stands for input voltage.

Also, it is possible to derive voltage equations of the other PWM modes using same method.

D. System Matrix

The backward difference method is adopted to treat the time derivative terms in the circuit voltage equations. After all, the system matrix can be constructed by combining the circuit voltage equations with the discretized governing equation.

In the case there is only main mesh current I_1 as shown in Fig. 4(c) and (d), the system matrix can be expressed as (6).

$$\begin{bmatrix} [S] & \{Q\} \\ \lfloor F \rfloor/\Delta t & 2R+2L_l/\Delta t \end{bmatrix} \begin{bmatrix} \{A\}^{t+\Delta t} \\ I_1{}^{t+\Delta t} \end{bmatrix} = \begin{bmatrix} [0] & \{0\} \\ \lfloor F \rfloor/\Delta t & 2L_l/\Delta t \end{bmatrix} \begin{bmatrix} \{A\}^{t} \\ I_1{}^{t} \end{bmatrix} + \begin{bmatrix} \{G\}^{t+\Delta t} \\ V_S{}^{t+\Delta t} \end{bmatrix} \quad (6)$$

where, S is the stiffness matrix, Q and F are the matrix related to the stator winding and BEMF, respectively. G is the forcing term by a magnet.

In the case of having two circuit voltage equations as shown in Fig. 4(a) and (b), the system matrix can be obtained as follows:

$$\begin{bmatrix} [S] & \{Q_1\} & \{Q_2\} \\ \lfloor F_1 \rfloor/\Delta t & 2R+2L_l/\Delta t & R+L_l/\Delta t \\ \lfloor F_2 \rfloor/\Delta t & R+L_l/\Delta t & 2R+2L_l/\Delta t \end{bmatrix} \begin{bmatrix} \{A\}^{t+\Delta t} \\ I_1{}^{t+\Delta t} \\ I_2{}^{t+\Delta t} \end{bmatrix} = \begin{bmatrix} [0] & \{0\} & \{0\} \\ \lfloor F_1 \rfloor/\Delta t & 2L_l/\Delta t & L_l/\Delta t \\ \lfloor F_2 \rfloor/\Delta t & L_l/\Delta t & 2L_l/\Delta t \end{bmatrix} \begin{bmatrix} \{A\}^{t} \\ I_1{}^{t} \\ I_2{}^{t} \end{bmatrix} + \begin{bmatrix} \{G\}^{t+\Delta t} \\ V_{S1}{}^{t+\Delta t} \\ V_{S2}{}^{t+\Delta t} \end{bmatrix} \quad (7)$$

V_S, V_{S1} and V_{S2} in (6) and (7) mean the voltage. Table I shows its values.

TABLE I
VOLTAGE VALUE OF (6) AND (7)

Case		V_S	V_{S1}	V_{S2}
Fig. 4	(a)		V_d -2V_{CE}	-(V_{CE}+V_F)
	(b)		-(V_{CE}+V_F)	-(V_{CE}+V_F)
	(c)	V_d -2V_{CE}		
	(d)	-(V_{CE}+V_F)		

IV. RESULTS AND DISCUSSIONS

To produce the PWM pulse patterns, we used a digital signal processor (DSP) installed controller and performed the experiment. Fig. 8 shows the prototype BLDCM with ferrite magnet. Fig. 9 and 10 compare the measured and the calculated BEMF and phase current in U_ON-L_PWM mode. The experimental results closely match those obtained from the simulation of the proposed analysis method.

There is difference between the phase current of each PWM modes as shown in Fig. 11. It is because how fast the open phase current decay to zero at commutation instant. The open phase current quickly diminishes in the ON_PWM mode because $-V_{dc}$ is connected to the voltage equation when the transistor switches off. This difference also has an effect on torque ripples. As shown in Fig. 12, the ON_PWM mode has higher torque ripple and lower average torque at the same input voltage. Accordingly, it is more advantageous to choose the PWM_ON mode in the BLDCM control system.

V. CONCLUSIONS

A 2-dimensional time-stepped voltage source finite element method taking account of the PWM mode in control system has been proposed in this paper. To prove the validity of the proposed analysis method, an experiment with a prototype BLDCM and DSP installed drive system was done and the results were compared with the analysis results. From the analysis and experimental results, it has been shown that accurate solutions can be obtained by the proposed method and the PWM_ON mode has a merit in terms of torque ripple and average torque.

We confirm that our analysis method would be useful for the design of the BLDCM with PWM mode control system.

REFERENCES

[1] S. Kitamura, "Magnetic field analysis of DC brushless motor considered volt-ampere characteristic of feedback diodes," *Inst. Electr. Engs. Japan*, vol. 12, pp. 1268-1275, 1996.

[2] T. J. E. Miller, *Brushless Permanent-Magnet and Reluctance MotorDrives*. Clarendon Press, 1989.

[3] Z. Xiangjun and C. Boshi, "Influences of PWM mode on the current generated by BEMF of switch-off phase in control system of BLDC motor," *International Conference ICEM 2001*, pp. 579-582, 2001.

[4] T. W. Preston, "Induction motor analysis by time-stepping techniques," *IEEE Transaction on Magnetics*, Vol. 24, No. 1, Jan 1988.

[5] F. Hecht, A. Marrocco, "A finite element simulation of an alternator connected to a non-linear external circuit," *IEEE Transaction on Magnetics*, Vol. 26, No. 2, March 1990.

[6] T. H. Kim and J. Lee, "Influences of PWM Mode on the Performance of Flux Reversal Machine," *IEEE Transaction on Magnetics*, vol. 41, no. 5, pp. 1956-1959, May 2005.

[7] T. H. Kim, S. H. Won, and J. Lee, "Finite Element Analysis of Flux-Reversal Machine Considering BEMF Current of a Switch-Off Phase and v-i Characteristics of a Transistor and a Freewheeling Diode," *IEEE Transaction on Magnetics*, vol. 42, no. 4, pp. 1039-1042, April 2006.

[8] S. Ogasawara and H. Akagi, "An approach to position senseless drive for brushless dc motors," *IEEE Transaction on Industry Applications*, vol. 27, no. 5, pp. 928-933, September/October 1991.

Fig. 8. The prototype BLDCM.

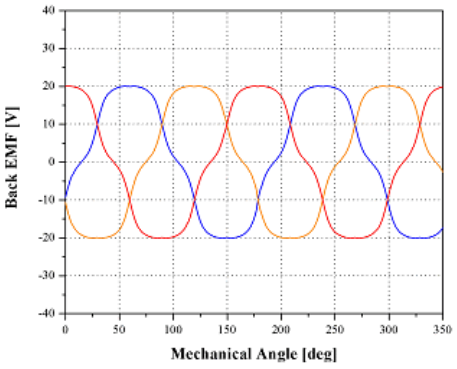

(a) Simulation

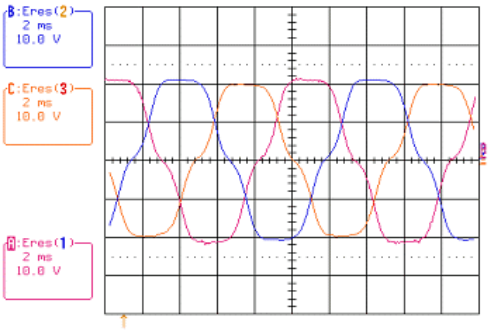

(b) Experimental

Fig. 9. BEMF waveforms.

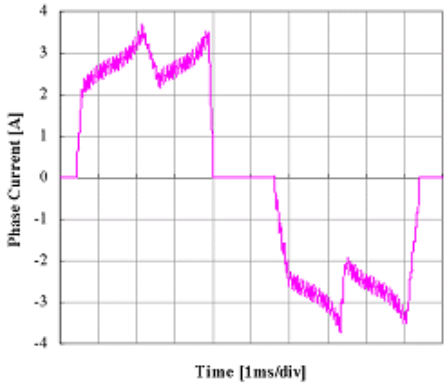

(a) Simulation

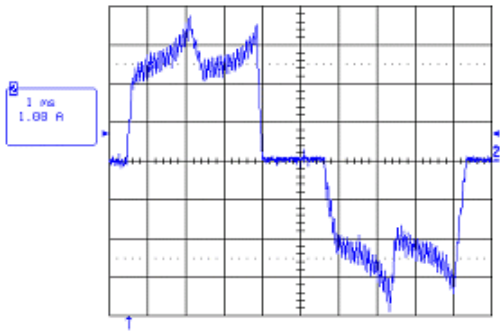

(b) Experimental

Fig. 10. Phase current waveforms in the U_ON-L_PWM mode.

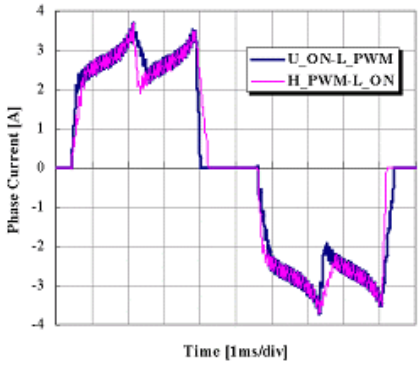

(a) U_ON-L_PWM and U_PWM-L_ON mode

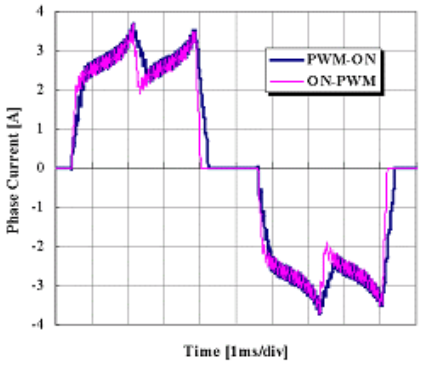

(b) PWM-ON and ON-PWM mode

Fig. 11. The comparison of phase current waveforms.

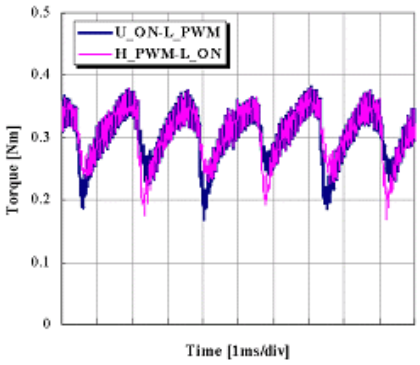

(a) U_ON-L_PWM and U_PWM-L_ON mode

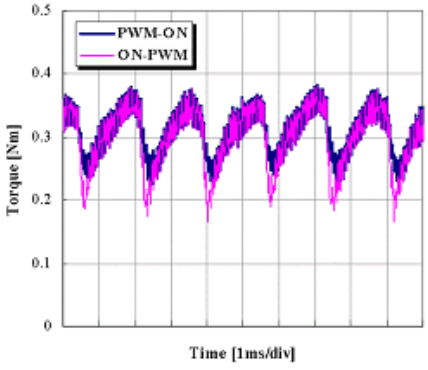

(b) PWM-ON and ON-PWM mode

Fig. 12. The comparison of torque ripples.